DOI:10.1021/jf9039099

JOURNAL OF AGRICULTURAL AND FOOD CHEMISTRY
ARTICLE

Compositional Changes in Cell Wall Polysaccharides from Japanese Plum (*Prunus salicina* Lindl.) during Growth and On-Tree Ripening

Nora M. A. Ponce,[†,§] Víctor H. Ziegler,[‡] Carlos A. Stortz,*[,†,§] and Gabriel O. Sozzi[‡,§]

[†]Departamento de Química Orgánica-CIHIDECAR, Facultad de Ciencias Exactas y Naturales, Universidad de Buenos Aires, Ciudad Universitaria, Pabellón 2, C1428 Buenos Aires, Argentina, and [‡]Departamento de Producción Vegetal, Facultad de Agronomía, Universidad de Buenos Aires, Avenida San Martín 4453, C1417 Buenos Aires, Argentina. [§] Research Member of the Consejo Nacional de Investigaciones Científicas y Técnicas (CONICET), Argentina.

Climacteric Japanese plums were harvested at six developmental stages with no intermediate storage period, and cell wall compositional changes were analyzed. Arabinose proved to be the principal neutral monosaccharide constituent in cell walls during growth and the most dynamic neutral sugar in pectic fractions. Arabinose loss from tightly bound pectins was found to be a relatively early feature in the sequence of cell wall biochemical modifications, thus suggesting a softening-related role during Japanese plum on-tree ripening. Depolymerization of matrix glycans started at the end of the cell expansion phase and increased throughout ripening. Pectin solubilization was first detected during early ripening. Firmness loss did not correlate with polyuronide depolymerization early in ripening, but the last softening phase was associated with a strong depolymerization of cell wall polyuronides as well as a decrease in the arabinose/galactose ratio in loosely bound pectins. This is the first work that characterizes the temporal sequence of cell wall polysaccharide changes in Japanese plum.

KEYWORDS: Cell wall degradation; pectin depolymerization; matrix glycan depolymerization; fruit softening; Prunoideae

INTRODUCTION

Plums are the most taxonomically diverse of stone fruits (*1*). There are about 42 species of plums, but most commercial plums currently grown are classified into one of two groups: the hexaploid ($2n = 6x = 48$) European type (primarily *Prunus domestica* L.) and the diploid ($2n = 2x = 16$) Japanese or Asian type (*Prunus salicina* Lindl.). Other types include damsons, mirabelles, bullaces, and 'St. Julien' (*P. domestica* L. ssp. *insititia*), which are small wild plums native to Europe. The bulk of the mirabelle and damson plum production is employed in the manufacture of jams, jellies, canned fruit, juices, and alcoholic drinks, whereas 'St. Julien' types are used primarily as dwarf rootstocks.

Although some European plums are consumed fresh (mainly if a very sweet fruit is desired), they usually display a relatively high sugar content so that they can be dried with the stony endocarp intact, being referred to as "prunes". This term can be applied both to the dried and the fresh product, but in the United States and in most countries they are usually eaten dried. On the other hand, Japanese plums are largely grown for fresh consumption and are regarded as the most common fresh market plums in the United States. Most of them are the result of extensive breeding. Genetic improvement of Japanese plums includes the achievement of high-quality fruit with long storage life (*2*). Japanese plum firmness, usually measured with a penetrometer fitted with a 7.9 mm tip, is one of the most important indices of plum quality and a good predictor of its potential shelf life. In general, Japanese plums may arrive at the warehouse at about 35−52 N and should be ripened to 18−22 N before being transferred to stores or restaurants. Premature plum softening to a ready-to-eat stage (6−13 N) virtually leads to a rapid deterioration during storage and an increased susceptibility to pathogens and mechanical injury.

Fruit softening is a multifaceted process resulting from a plethora of changes at a morphological and cellular level, chiefly cell wall disassembly and reduction of turgor pressure. During fruit growth, fruit cells withstand strong pressures and require maintenance of cell wall strength plus control of the wall loosening and continued integration of new structural polymer components into the wall (*3*). During ripening, the disassembly of cell wall architecture is associated with degradation of its polysaccharides and modification of linkages between polymers. In addition, turgor pressure drops because of the accumulation of solutes in the cell wall space and contributes to textural changes during ripening (*4*).

*Corresponding author [telephone/fax (+5411)-4576-3346; e-mail stortz@qo.fcen.uba.ar].

 Published on Web 01/25/2010

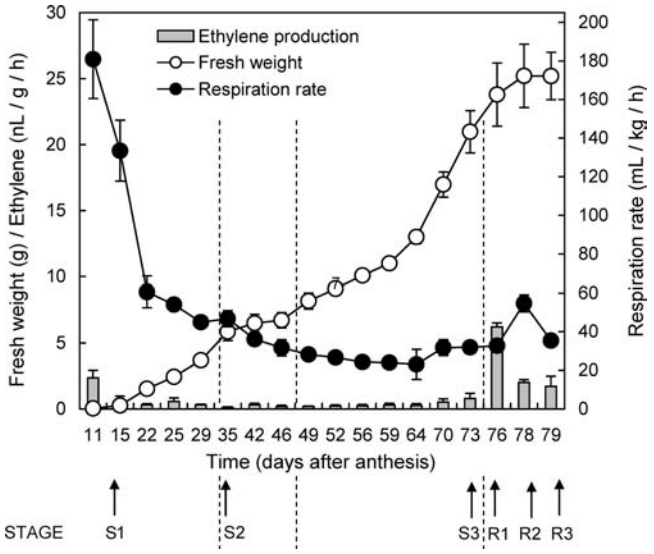

Figure 1. Fruit weight, ethylene production, and respiration rate of the 'Gigaglia' plum fruit during development and on-tree ripening. Values represent the means ± SE (n = 20 for fruit weight; n = 3 for ethylene production and respiration rate). Where bars are not shown, the SE does not exceed the size of the symbol. Stages were designated as follows: S1, initial phase of exponential growth; S2, lag phase; S3, cell expansion phase (preripe or preclimacteric fruit). Ripening stages were designated as follows: R1, early ripe (peak ethylene production); R2, midripe; R3, fully ripe. Arrows indicate the sampling dates for cell wall analyses.

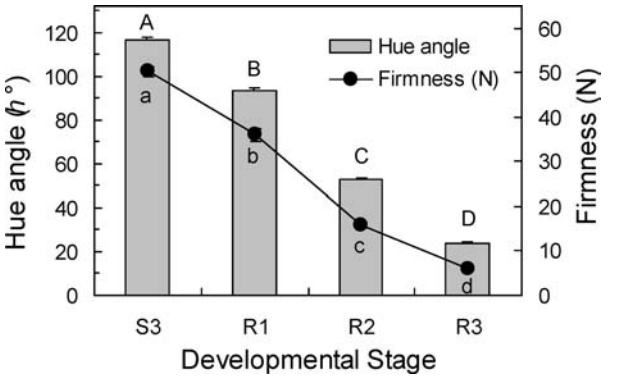

Figure 2. Hue angle (h°) and firmness (N) of the 'Gigaglia' plum. Values represent the means ± SE (n = 20). Where bars are not shown, the SE does not exceed the size of the symbol. Different capital letters (hue angle) or small letters (firmness) indicate significant (p < 0.05) differences between stages.

The structure of fruit cell walls has not been fully elucidated, but the complexity of its disassembly involves the dismantling of multiple polysaccharide networks during softening (*4*−*6*). Detailed comparisons on cell wall polymer metabolism among different species have furthered much of the current knowledge about fruit softening and support the unfeasibility of considering that a particular species or cultivar could be a "model" applicable to other related species (*4*). In fact, major differences in cell wall polysaccharide changes have already been detected at a genus level in some major tree fruit crops such as *Pyrus* spp. (*7*) and *Prunus* spp. (*8*, *9*).

Some peaches and plums undergo considerable softening and achieve a smooth melting texture when ripe. This is thought to be mainly due to a regulated dismantling of the primary cell wall. Pectin solubilization is relatively important in peaches, nectarines, and plums (*10*−*12*). Besides, the loss of some neutral sugars, mainly Gal and Ara, is considered to be a common trait of fruit ripening in general (*8*) and of peaches in particular (*10*).

Plums have been considered an exception as no loss of polymeric Gal or Ara has been detected during ripening (*4*). In fact, this statement is based on previous studies (*8*, *13*) carried out on "prunes" (*P. domestica* L.), which are not primarily grown for fresh consumption. Most of the literature in this area is related to the cell wall compositional changes of European plums (see ref *14* and references cited therein) and wild plums, *P. domestica* L. ssp. *insititia* (*9*). Only a few papers studied particular aspects of the cell wall in Japanese plums. Taylor et al. (*15*) and Manganaris et al. (*16*) addressed the influence of chilling injury on the pectic fractions of *P. salicina* Lindl. fruit cell wall. When comparing 'Reine Claude' (*P. domestica* L.), 'Prune Rouge' (*P. salicina* Lindl.), and 'Golden Japan' (*P. salicina* Lindl.), Renard and Ginies (*14*) found that intraspecific cell wall compositional differences could be more important than interspecific variations. In these works, Japanese plums sampled at a commercial maturity stage were used. However, other events involved in Japanese plum cell wall assembly and disassembly during development have not yet been analyzed in detail. The aim of this work is to characterize the temporal sequence of cell wall polysaccharide changes during normal growth and on-tree ripening of Japanese plums.

MATERIALS AND METHODS

Plant Material. 'Gigaglia' plum samples were randomly picked from the orchard of the Facultad de Agronomía, Universidad de Buenos Aires (34° 35′ 43″ S; 58° 29′ 04″ W). 'Gigaglia' is an early hybrid, Japanese-type plum, involving a cross to *P. salicina* Lindl. Trees were grown on Myrobalan plum rootstocks and trained to an open-vase system. Japanese plums were submitted to standard cultural practices including pruning, fruit thinning, fertilization, irrigation, and pest control.

During growth, plums were harvested at different physiological stages, and their age (days after anthesis, DAA), weight, ethylene production, and respiration rate were registered (**Figure 1**). During growth, cell wall analysis was performed at the following stages: S1, initial phase of exponential growth (15 DAA); S2, lag phase (35 DAA); S3, end of the cell expansion phase, preripe or preclimacteric (73 DAA, firmness = 50 N). During on-tree ripening and softening, fruits were collected at each of three developmental stages on the basis of flesh firmness, color, and ethylene production (**Figures 1** and **2**), as follows: R1, early ripe (76 DAA, firmness ∼36 N); R2, midripe (78 DAA, firmness ∼ 18 N); R3, fully ripe (79 DAA, firmness ∼ 6 N). Plums were harvested for measurement of these indices, sampled, and immediately frozen in liquid nitrogen for cell wall extraction.

Ethylene Production, Respiration Rate, Color, and Firmness Assessment. Ethylene production was assessed by placing the plums in a 1.5 L glass container tightly sealed with a lid carrying a silicone septum. One milliliter of the headspace gas was extracted after 1 h at 20 °C. Ethylene was quantified on a Hewlett-Packard 5890 series II gas chromatograph (Agilent Technologies, Inc., Santa Clara, CA) as described elsewhere (*17*). The column used was a stainless steel, 2 m × 3.2 mm i.d., 80/100 mesh Porapak N (Supelco Inc., Bellefonte, PA). The injector, oven, and detector (FID) temperatures were 110, 90, and 250 °C, respectively. Nitrogen was used as the carrier gas at a flow rate of 22 mL/min. Three independent composite (5 g for S1, 20 g for S2, and 100 g for S3−R3) samples per developmental stage were evaluated.

Gas samples for ethylene and CO_2 analyses were collected from the same jars. The respiration rate was quantified on an Agilent 4890 gas chromatograph (Agilent Technologies, Inc.) as previously described (*18*). The column used was a 25 m × 0.53 mm i.d., 25 μm, CP-Carboplot (Varian Argentina Ltd., Buenos Aires, Argentina). The analysis was performed isothermally at 100 °C, with the injector and the detector (TCD) temperatures at 80 and 200 °C, respectively. Helium was used as the carrier gas at a flow rate of 9 mL/min. Three independent composite (5 g for S1, 20 g for S2, and 100 g for S3−R3) samples per developmental stage were evaluated.

Table 1. Uronic Acid Content (Milligrams per Gram of AIR) in Cell Wall Fractions of the 'Gigaglia' Plum at Developmental Stages S1−R3[a]

	stage					
cell wall fraction	S1	S2	S3	R1	R2	R3
W-F	8.7 ± 0.4 d	9.2 ± 0.4 d	13.1 ± 0.6 c	65.7 ± 2.0 b	69.8 ± 3.6 b	114.7 ± 3.7 a
CDTA-F	26.3 ± 1.1 f	38.9 ± 1.0 e	60.1 ± 2.8 c	116.9 ± 5.4 a	71.7 ± 6.2 b	47.9 ± 1.7 d
Na_2CO_3-F	86.7 ± 2.1 c	90.3 ± 3.6 c	85.9 ± 3.7 c	131.8 ± 7.6 b	152.2 ± 2.9 a	57.7 ± 1.2 d
4% KOH-F	9.0 ± 0.4 c	12.4 ± 0.3 a	7.4 ± 1.0 d	11.2 ± 0.5 b	5.2 ± 0.8 e	9.3 ± 0.5 c
24% KOH-F	8.3 ± 0.4 a	5.7 ± 0.5 b	1.5 ± 0.1 e	nd[b]	3.1 ± 0.3 c	2.2 ± 0.2 d

[a] Values represent the means ± SD ($n = 3$). Different letters within each cell wall fraction (row) indicate significant ($p < 0.05$) differences between stages. [b] nd, not determined.

Hue angle ($h°$) values were measured on the equatorial region of intact fruit with a model CR-300 chromameter (Minolta, Osaka, Japan) using CIE illuminant C lighting conditions and an 8 mm diameter measuring area (*19*). The chromameter was calibrated to a white calibration plate (CR-A43). Two opposite spots at the equatorial plane of the fruit were measured, and the mean of the two measurements was considered as one replicate. Twenty independent samples per developmental stage were evaluated.

Whole-fruit firmness (flesh rupture force) was determined in puncture tests by measuring the force required to penetrate each plum, with the skin removed, to a depth of 8 mm using an Instron Universal Testing Machine model 4442 (Instron Corp., Canton, MA). Each fruit was placed on a stationary steel plate. Two opposite spots at the equatorial plane of the fruit were punctured. Tests involved the use of a convex probe 7.9 mm in diameter on a drill base with a crosshead setting of 50 mm/min, as previously described (*19*). Twenty independent samples per developmental stage were evaluated.

Cell Wall Preparation and Fractionation. After removal of the endocarp, Japanese plums were sliced into pieces, frozen immediately in liquid nitrogen, and stored at −50 °C until used. Cell wall preparation was performed as previously described (*20*) with slight modifications: 20 g was dropped into 80 mL of ice-cold 80% ethanol and homogenized in a Waring blender and an Omni Mixer homogenizer (Omni International, Kennesaw, GA). The homogenate was immediately boiled for 30 min, then allowed to cool down, and filtered through glass filter paper (Whatman GF/C). The retentate was thoroughly washed with 95% ethanol. The solids were then resuspended in 60 mL of chloroform/methanol (1:1), stirred during 15 min and filtered. The retentate was washed with 40 mL of the same solvent mixture. The insoluble material was washed with acetone until decolorized, yielding the crude cell wall extract (alcohol insoluble residue, AIR). The AIR was air-dried in a hood and in a vacuum desiccator overnight and then weighed.

Cell wall fractionation was performed as previously described (*20*), with slight modifications. Briefly, 3 g of AIR was stirred for 24 h at room temperature with 300 mL of 0.02% (w/v) thimerosal aqueous solution and filtered. The supernatant, designated water-soluble fraction (W-F), was removed. Sequential extraction of the pellet with 0.05 M CDTA in 0.05 M NaOAc/HOAc buffer, pH 6, containing 0.02% (w/v) thimerosal (24 h), 0.1 M Na_2CO_3 in 0.1 mM $NaBH_4$ (24 h), 4% KOH in 0.1% (w/v) $NaBH_4$ (24 h), and 24% KOH in 0.1% (w/v) $NaBH_4$ (24 h), produced the CDTA-soluble fraction (CDTA-F), Na_2CO_3-soluble fraction (Na_2CO_3-F), and 4 and 24% KOH-soluble fractions (4% KOH-F and 24% KOH-F), respectively. The supernatants were recovered after centrifugation at 13100*g*. In the case of the 4 and 24% KOH-F, the pH was adjusted to 5 with glacial CH_3COOH. All fractions were dialyzed (M_w cutoff 6000−8000) exhaustively against tap water for 2 days and against distilled water for another day at 4 °C. The volume of each dialysate was recorded, and fractions were recovered by lyophilization.

Uronic Acid, Total Carbohydrate, and Neutral Sugar Measurements. Uronic acids were quantified according to the *m*-hydroxybiphenyl method (*21*) using GalA as the standard and expressed as anhydro units. Total carbohydrates were determined according to the phenol−H_2SO_4 method (*21*) using Glc as the standard. The proportion of neutral sugars was determined after subtraction of the uronic acid content from that of total carbohydrates. For this purpose, the phenol−H_2SO_4 reaction was also carried out with a GalA standard, which showed an absorbance ratio of 0.28 against the same Glc weight.

Size Exclusion Chromatography (SEC). To examine the size distributions of polymers in the W-F, the extracts were redissolved in 50 mM $NaNO_3$ and fractionated by high-pressure SEC on a LKB-HPLC (Pharmacia, Uppsala, Sweden) equipped with a 2150 pump and a model RID-10A refractometer index detector (Shimadzu Corp., Tokyo, Japan). Four columns were used in series, as follows: 300 mm × 7.8 mm i.d. Poly Sep-GCF-P 5000 (Phenomenex, Torrance, CA), Progel-TSK G4000 PWXL (Supelco Inc.), Ultrahydrogel 120 and Ultrahydrogel 250 (Waters Corp., Milford, MA) as well as a 40 mm × 6 mm i.d. Progel-TSK PWXL guard column. Elution was carried out at a flow rate of 0.7 mL/min with 50 mM $NaNO_3$ containing 0.02% NaN_3 as a bactericide. The solutions were solubilized under magnetic stirring and then filtered through a 0.22 μm membrane filter (Millipore Co., Bedford, MA).

Samples from the CDTA-F and Na_2CO_3-F were dissolved in 0.8 mL of 0.4 mg/mL imidazole to which 0.2 mL of 1 M NH_4AcO (pH 5) was added. Solutions were cleaned up by centrifugation and chromatographed on a low-pressure SEC by employing a 300 mm × 9 mm i.d. Sepharose CL-2B column (Sigma Chemical Co., St. Louis, MO) eluted at room temperature with 0.2 M NH_4AcO, pH 5 (*10*). Samples from the 4 and 24% KOH-F were dissolved in 0.1 M NaOH, cleaned up by centrifugation, and chromatographed on a low-pressure SEC by means of a 300 mm × 9 mm i.d. Sepharose CL-6B column (Sigma Chemical Co.) eluted at room temperature with 0.1 M NaOH. Fractions were collected and, with a pectin fraction, aliquots were assayed for total carbohydrates and for uronic acids (*21*), showing very similar profiles for both assay methods. Therefore, only results for total carbohydrates are shown.

Neutral Sugar Composition. Each fraction (ca. 3 mg) was hydrolyzed with 2 M trifluoroacetic acid (TFA, 1 mL) for 90 min at 120 °C in closed-cap vials. The TFA was eliminated by evaporation, and the resulting monosaccharides were reduced to alditols using $NaBH_4$ and converted to alditol acetates (*21*), which were analyzed using a Hewlett-Packard 5890 gas chromatograph (Agilent Technologies, Inc.) fitted with a capillary column 30 m × 0.25 mm i.d. 0.20 μm, SP-2330 (Supelco Inc.) and equipped with a FID operated at 240 °C. The injector temperature was 240 °C, and the oven temperature was kept isothermally at 220 °C. Nitrogen was used as the carrier gas at a flow rate of 1 mL/min. Aliquots were injected with a split ratio of ca. 80:1. *myo*-Inositol was used as the internal standard, and the different alditol acetates were identified by comparison with authentical standards. The percentage of the different monosaccharides was calculated by considering that the FID responses are proportional to the molecular weight of the alditol acetates.

Statistical Analysis. For ethylene production, respiration rate, firmness, $h°$, uronic acid content, and neutral sugar content, statistical significance was determined by one-way ANOVA with the PC-SAS software package (SAS Institute Inc., Cary, NC). The model assumptions of homogeneity of variance and normality were probed by means of Levene's and Shapiro−Wilk's tests, respectively. When these assumptions were not satisfied, data were transformed into ranks for further analysis. When a significant F value was found, treatment means were compared using Tukey's studentized range test ($p < 0.05$).

RESULTS

Fruit Characterization. A series of Japanese plum fruit stages was chosen, based on fruit weight, ethylene production, epicarp color, and firmness (**Figures 1** and **2**). In attached fruit, the first period of rapid growth lasted ∼32 days and pit hardening occurred between days 32 and 46 (**Figure 1**). The second stage of rapid growth, which is primarily a function of cell expansion, finished ∼76 DAA, when the first color change was attained (**Figure 2**). 'Gigaglia' plum showed a typical climacteric pattern

Table 2. Neutral Sugar Content[a] (Milligrams per Gram of AIR) in Cell Wall Fractions of the 'Gigaglia' Plum at Developmental Stages S1−R3[b]

	stage					
cell wall fraction	S1	S2	S3	R1	R2	R3
W-F	10.5 ± 0.5 d	13.3 ± 0.5 c	10.3 ± 0.5 d	12.2 ± 1.1 c	34.6 ± 1.9 b	96.7 ± 3.0 a
CDTA-F	17.4 ± 1.1 c	11.3 ± 1.0 d	30.7 ± 2.8 b	12.6 ± 3.3 cd	16.3 ± 3.3 c	39.6 ± 1.1 a
Na_2CO_3-F	60.0 ± 3.9 d	34.7 ± 2.1 f	73.7 ± 2.3 c	99.2 ± 6.9 a	82.2 ± 2.9 b	42.3 ± 0.6 e
4% KOH-F	30.7 ± 0.7 d	41.5 ± 0.4 b	41.0 ± 2.2 b	50.4 ± 1.1 a	43.3 ± 1.7 b	34.6 ± 0.7 c
24% KOH-F	73.2 ± 2.4 a	55.3 ± 1.8 b	42.3 ± 0.4 d	nd[c]	47.8 ± 2.3 c	43.0 ± 1.2 d

[a] Obtained after subtracting the content of uronic acids from that of total carbohydrates (see Materials and Methods. [b] Values represent the means ± SD (n = 3). Different letters within each cell wall fraction (row) indicate significant (p < 0.05) differences between stages. [c] nd, not determined.

Table 3. Neutral Sugar Composition (Moles per 100 mol) of Pectin and Glycan Matrix Fractions of the 'Gigaglia' Plum in Each of the Six Developmental Stages

		monosaccharide						
fraction	stage	Rha	Fuc	Ara	Xyl	Man	Gal	Glc
W-F	S1	6	tr	44	9	2	36	3
	S2	4	tr	40	20	4	28	4
	S3	5	1	36	10	6	42	–
	R1	11	1	42	10	3	32	1
	R2	6	1	30	10	5	40	7
	R3	8	tr	36	3	2	48	3
CDTA-F	S1	7	tr	46	2	2	41	2
	S2	7	tr	60	1	1	29	tr
	S3	12	1	62	1	–	24	–
	R1	9	tr	66	1	–	24	–
	R2	12	1	50	9	tr	26	tr
	R3	9	1	37	2	1	48	2
Na_2CO_3-F	S1	6	–	72	1	–	21	–
	S2	7	–	70	tr	–	22	–
	S3	7	–	37	–	–	56	–
	R1	6	tr	50	1	–	43	–
	R2	7	tr	30	tr	–	62	–
	R3	8	tr	39	tr	1	52	tr
4% KOH-F	S1	3	1	29	17	1	41	8
	S2	4	1	29	15	2	38	11
	S3	3	2	23	17	2	42	11
	R1	3	2	27	15	1	39	13
	R2	3	2	25	20	2	36	11
	R3	3	2	32	23	3	25	12
24% KOH-F	S1	2	3	14	22	4	28	27
	S2	2	4	15	30	7	19	23
	S3	1	5	10	31	8	15	30
	R1	1	4	8	30	6	18	33
	R2	1	3	13	24	7	24	28
	R3	1	5	10	29	5	17	33

with significant (p < 0.05) ethylene production and respiration rate peaks at R1 and R2, respectively (**Figure 1**). This climacteric is typically associated with firmness loss, resulting in rapid perishability. Significant (p < 0.05) fruit softening occurred between S3 and R3 at a rate of 7 N/day and was paralleled by a major drop in $h°$ from 117 to 23 (**Figure 2**).

Pectin Solubilization, Depolymerization, and Composition. An upsurge in the relative solubility of pectins was associated with shifts in the uronic acid contents of the three pectin-rich fractions, which denoted an increase in the ease of extractability (**Table 1**). A noticeable augmentation in the proportion of pectin that became water-soluble was detected as ripening progressed. A reciprocal decrease was measured in the proportions of CDTA-F between R1 and R3, whereas the amount of uronic acids in the Na_2CO_3-F dropped at more advanced stages of development, between R2 and R3 (**Table 1**). This was accompanied by an increase in Japanese plum neutral sugars in the W-F and CDTA-F and a concomitant drop in the Na_2CO_3-F during ripening (**Table 2**).

As depicted in **Table 3**, the composition of loosely (W-F), ionically (CDTA-F), and tightly bound (Na_2CO_3-F) pectins proved to be rich in Ara and Gal and, to a lesser extent, Rha. Other neutral sugars such as Xyl, Man, and Glc were also present in the W-F but hardly noticeable in the CDTA-F and Na_2CO_3-F. The amount (mol %) of Ara quantified in the CDTA-F and Na_2CO_3-F generally showed a pattern opposite to that found for Gal, thus suggesting a net loss of Ara and a relative increase in Gal during growth and on-tree ripening. This is even better shown in **Figure 3**, where the Ara/Gal and the (Ara + Gal)/Rha ratios were determined for every fraction and stage. The first ratio determines the relative importance of Ara and Gal side chains in pectins, and the second one estimates the relative importance of "total" neutral side chains to the RG backbone (*14*).

In W-F no significant changes in polymer size distribution were observed (data not shown). In S1 and S2, CDTA-soluble polyuronide distribution showed a broad shoulder of mid- and low-size molecular mass, with low levels of high molecular mass species (**Figure 4**). This molecular weight profile changed gradually from S3 to R2, with a substantial increase in high molecular weight molecules. Finally, a drastic shift in the molecular weight profile occurred in R3 to a lower average M_r, with an almost complete loss of high molecular weight molecules and a partial loss of midsized polymers (**Figure 4**). Subsequent extraction with Na_2CO_3 released another set of polyuronide molecules, which eluted as a single peak of moderate molecular weight (**Figure 4**). Small amounts of high molecular weight carbohydrates were detected in Na_2CO_3-F from S1 to R2, although not in R3 (**Figure 4**).

Matrix Glycan Solubilization, Depolymerization, and Composition. Low amounts of uronic acids were detected in the two matrix glycan fractions (**Table 1**), thus suggesting that some neutral sugar-containing molecules in the 4 and 24% KOH-F are very tightly bound pectins. The proportion of neutral sugars in the 4% KOH-F increased during growth with a maximum in R1 and a subsequent decrease (**Table 2**). In the 24% KOH-F, maximum levels of neutral sugars were found in S1, decreasing during growth and remaining stable after reaching the S3 stage (i.e., throughout the on-tree ripening period).

SEC revealed that matrix glycans extracted in the 4% KOH-F were different with regard to molecular weight profile from those extracted in the 24% KOH-F. In S1, 4% KOH-F formed a very high molecular weight peak close to the exclusion limit of the column, with another increase in the amount of midsized matrix glycans (**Figure 5**). The amount of high molecular weight polymers eluting in the void of the column increased in S2, probably due to the integration of new structural hemicellulosic components into the wall, but fell at the end of the cell expansion phase (S3) when fruit was preclimacteric in terms of ethylene production. During R1 and R2, the relative amount of high molecular

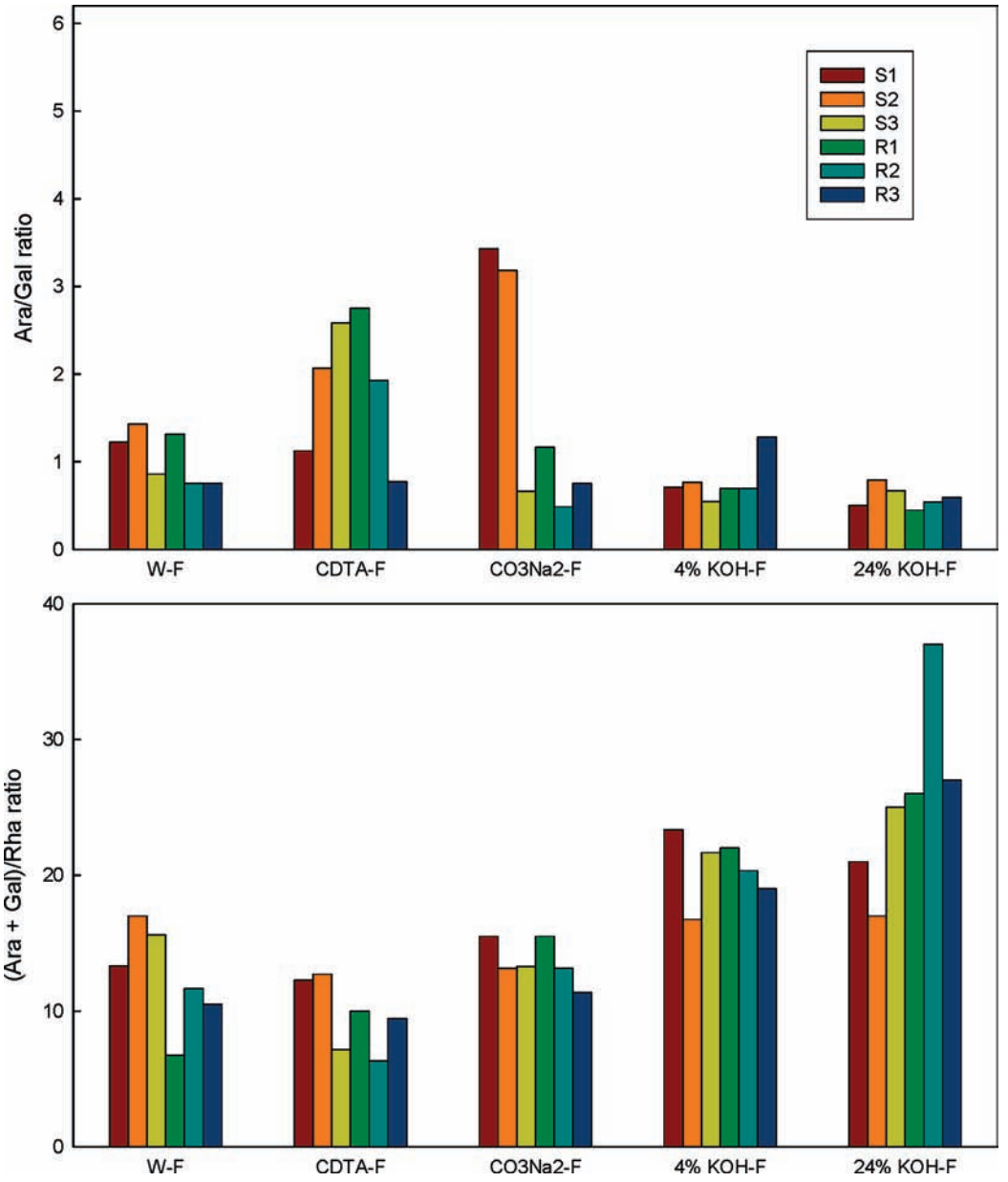

Figure 3. Ara/Gal and (Ara + Gal)/Rha ratios for cell wall pectins and matrix glycans. Contiguous bars represent the six developmental stages, in order, from left to right: S1, S2, S3, R1, R2, and R3.

weight glycans showed a further decline while the midsized polymers increased. At the R3 stage, the total amount of matrix glycans reached the lowest level and high molecular weight species were hardly noticeable.

The clear separation observed in the 4% KOH-F between peaks of high and mid molecular weight was not detected in the 24% KOH-F. In S1 fruit, tightly bound matrix glycans were spread more evenly throughout the separation rate of the column (**Figure 5**). Polymers remained polydisperse in S2, but a progressive downshift became apparent in S3. A drastic decrease in the relative amount of high molecular weight polymers occurred in R1, with a sharpening of a single major peak of moderate molecular weight that remained throughout on-tree ripening.

Loosely bound matrix glycans were found to be rich in Gal and Ara and, to a lesser extent, in Xyl and Glc, with a slight increase in the mole percent of Ara and Xyl during ripening (presumably due to the presence of an arabinoxylan) and a concomitant decrease in Gal. Glc showed little change throughout development, whereas Rha, Fuc, and Man were detected in negligible amounts. In contrast, tightly bound matrix glycans displayed high mole percent levels of Glc and Xyl (consistent with the presence of xyloglucans) and lower but still substantial percentages of Gal and Ara. Tightly bound matrix glycans also contained measurable levels of Man and Fuc. These sugars showed only slight changes throughout development and are typically associated with the presence of mannans or galactomannans and fucosylated xyloglucans.

DISCUSSION

'Gigaglia' is an early-maturing Japanese cultivar with a medium to high on-tree ripening rate (**Figures 1** and **2**). This early cultivar showed a ripening pattern typical of climacteric fruits. In climacteric Japanese plums, the increase in ethylene production has been shown to be associated with sharp increases of transcripts corresponding to different ethylene perception and signal transduction components: *Ps-ETR1*, *Ps-ERS1*, *Ps-CTR1*, and *Ps-ERF1* (*22*). Growth and on-tree ripening of 'Gigaglia' plum are accompanied by modifications both in the cell wall architecture

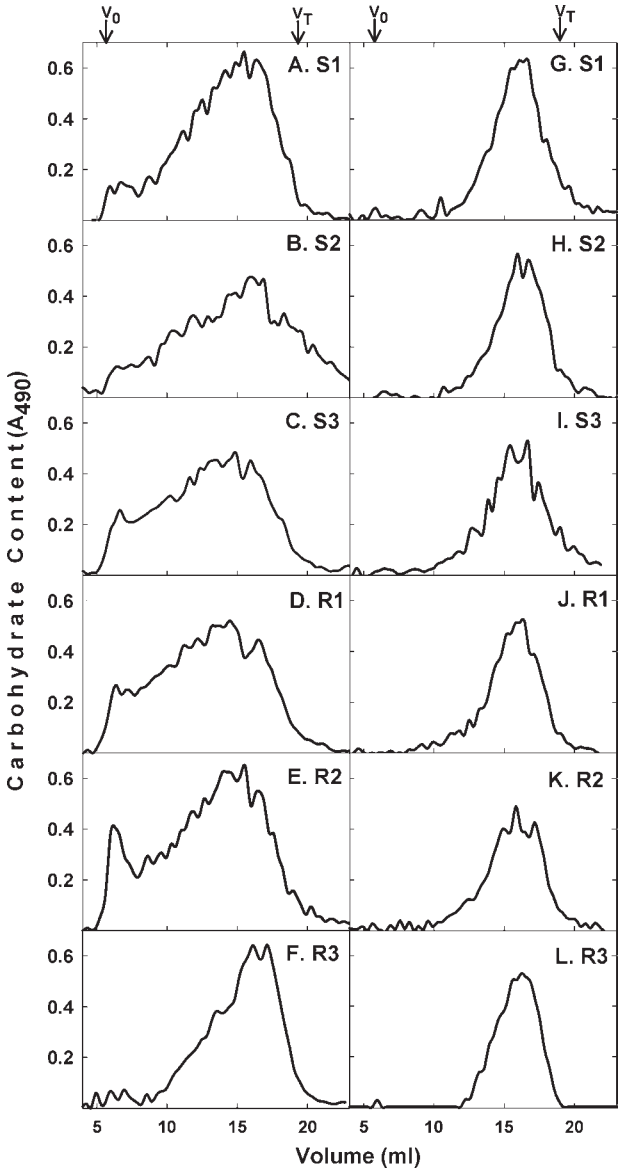

Figure 4. Size exclusion chromatography profiles from the 'Gigaglia' plum CDTA-F (**A**−**F**) and Na_2CO_3-F (**G**−**L**) throughout growth (S1−S3) and on-tree ripening (R1−R3), fractionated on a Sepharose CL-2B column. Column fractions were assayed as previously described (*21*). V_0, void volume; V_T, total volume.

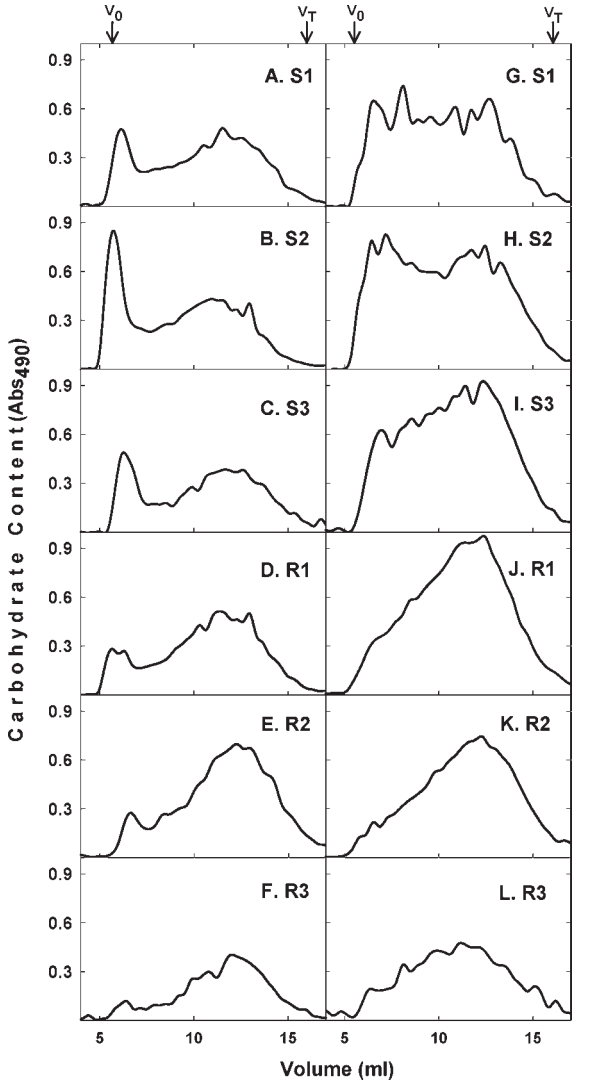

Figure 5. Size exclusion chromatography profiles from the 'Gigaglia' plum 4% KOH-F (**A**−**F**) and 24% KOH-F (**G**−**L**) throughout growth (S1−S3) and on-tree ripening (R1−R3), fractionated on a Sepharose CL-6B column. Column fractions were assayed as previously described (*21*). V_0, void volume; V_T, total volume.

and in the polymers composing it. The most important changes are the solubilization (**Table 1**) and depolymerization of polyuronides (**Figure 4**), the extensive depolymerization of matrix glycans (**Figure 5**), and the loss of Ara (**Table 3**; **Figure 3**).

The in vitro analysis of cell wall pectic polysaccharides from different fruit species has established that many of them undergo solubilization during ripening (*12*). Some fruit species soften to a melting texture during ripening (such as persimmon, tomato, strawberry, European plum, blackberry, kiwifruit, and avocado) and display a pronounced cell wall swelling that is usually accompanied by moderate to heavy pectin solubilization. In peach, increased pectin solubilization begins early in ripening and precedes detectable polyuronide depolymerization (*10*). In our work, increased pectin solubilization is indirectly shown by the enhanced capacity of some pectic polysaccharides to be extracted from isolated Japanese plum cell wall material by water (**Table 1**). An upsurge in W-F polyuronides possibly results from an increasing proportion of pectin molecules that are strongly held in the S3 fruit cell wall by ionic calcium bridges or covalent bonds and become weakly attached to the bulk of the wall during on-tree ripening.

Pectic polysaccharide depolymerization in 'Gigaglia' plums is confirmed by a lowering of the molecular mass (**Figure 4**), probably because of the cleavage of the rhamnogalacturonan backbone. Efficient degradation of polysaccharides can require synergistic interactions between enzymes responsible for cleaving the set of different polymer linkages. Access to pectin backbones is likely to be influenced by enzymes that remove polymer side chains, such as β-galactosidase/galactanase and α-arabinofuranosidase/arabinase (*5*, *20*). Therefore, some loss of neutral Gal-Ara side chains could contribute to lowering of the molecular mass. The enzyme-induced depolymerization is considered to be a general mechanism in fruit ripening, but the extent of this process greatly varies (*4*). The molecular weight of the solubilized pectins was shown to be similar in unripe and ripe European plum (*12*), but it undergoes a moderate reduction during tomato ripening (*23*) and a severe reduction during avocado ripening (*24*). In peach, little change was detected in midripe fruit as compared with unripe, but a drastic depolymerization was observed late

in ripening (*10*). In Japanese plum, a clear molecular weight downshift of the CDTA-soluble fraction has been observed at the fully ripe stage (**Figure 4F**). Conversely, tightly bound polyuronides in the Na_2CO_3-F showed little change in the molecular weight profile during Japanese plum on-tree ripening (**Figure 4G−L**), as previously reported for tomato (*23*), melon (*25*), and peach (*10*).

Depolymerization of matrix glycans is at least as important as that of pectic polymers in affecting the structural integrity of the cell wall (*4*). Many studies demonstrated the depolymerization of matrix glycans in different ripening tree fruits including avocado (*26*), kiwifruit (*27*), persimmon (*28*), and peach (*10*). In persimmon, depolymerization takes place only in tightly bound glycans (*28*). The Japanese plum resembles peach in that depolymerization occurs in both loosely bound and tightly bound matrix glycans (**Figure 5**) (*10*). In contrast with peach, depolymerization of loosely bound matrix glycans from 'Gigaglia' plums does not precede that of tightly bound matrix glycans (**Figure 5**). The characteristic pattern of M_r changes in 4% KOH-F from Japanese plums is similar to that observed in tomato fruit (*29*) because loosely bound matrix glycans fractionate on gel permeation columns into two M_r sets regardless the ontogeny stage tested. On the other hand, tightly bound matrix glycans from S1 and S2 Japanese plums are polydisperse, and a general shift to a lower average M_r is observed in S3, resembling that of 4 M alkali-soluble polysaccharides from avocado fruit (*26*). The broad range of tightly bound matrix glycans undergoes a shift to a lower average M_r in S3 and a decrease in polydispersity in early ripe plums, with the presence of a single major peak. In the later ripening stages, tightly bound matrix glycans form a predominant peak of midsize molecular mass with a very small amount of high molecular mass species. The most remarkable downshift of matrix glycans occurs in 24% KOH-F between the S3 and R1 stages, but a progressive depolymerization of glycans from 4 and 24% KOH-F begins in S3 and continues throughout on-tree ripening.

The removal of noncellulosic neutral sugars (mainly Gal and/or Ara) from the side chains is a mechanism of depolymerization of pectic polysaccharides that seems to be widespread in almost all fruit species (*8*). Nevertheless, Gross and Sams (*8*) did not detect relevant changes in Gal or Ara when comparing three different stages of European plums: immature green with nearly complete pit hardening, mature turning, and ripe and soft (corresponding approximately to S2, R1, and R3 in our study). Also, Redgwell et al. (*13*) found no loss of Gal or Ara between two developmental stages of European plum, physiologically mature and ripe (S3 and R3 in our study), although fruit showed moderate wall swelling, pectin solubilization, and considerable softening. In 'Gigaglia' plums, changes in the Ara/Gal ratio are particularly noticeable within the pectic fractions as the aging process occurs (**Figure 3**). A substantial loss of Ara and a conspicuous relative rise in Gal is more evident in the Na_2CO_3-F, generally assumed to be enriched for covalently bound pectins, at S3 (**Table 3**; **Figure 3**). Conversely, R1−R3 show an extensive decline in the Ara content from the CDTA-F, considered to be abundant for ionically bound pectins (**Table 3**; **Figure 3**). Gal was found to be the most abundant noncellulosic neutral monosaccharide in pectic polymers from ripe 'Fortune' and 'Golden Japan' Japanese plum flesh (*14*, *16*), being approximately twice as abundant as Ara. On the other hand, 'Prune Rouge' Japanese plum pectic fractions showed Ara/Gal ratios closer to 1 (*14*). Gal is also the principal monosaccharide in fully ripe 'Gigaglia' plums, although Ara is found to be the most important at the beginning of Japanese plum ontogeny, comprising > 70% of total neutral sugars in ionically and covalently bound pectins during S1 (**Figure 3**). In any case, results for fully ripe 'Gigaglia' plum regarding the Ara/Gal ratio resemble more closely those found for 'Prune Rouge' than those for 'Fortune' and 'Golden Japan' varieties (*14*, *16*). Ara proved to be the most dynamic neutral sugar in pectic fractions from 'Gigaglia' plums in contrast with previous findings in other species from the same genus, such as *P. domestica* L. (*8*, *13*) and *Prunus persica* (L.) Batsch (*10*). In pectic fractions, Ara and Gal are usual constituents of branched arabinans, branched arabinogalactans, and linear galactans of the rhamnogalacturonan-I. Also, the (Ara + Gal)/Rha ratio does not show large variations with onthogeny, although a small decrease in this index occurs for W-F and Na_2CO_3-F (**Figure 3**). Values for this index are lower than those observed previously for other varieties (*14*), suggesting that the pectins of 'Gigaglia' plums are less branched than those of 'Prune Rouge' or 'Golden Japan' plums.

Interestingly, Ara is also present in matrix glycans (**Figure 3**). Ara slightly decreased in 4% KOH-F during S3 but increased during on-tree ripening, whereas Gal decreased and the Ara/Gal ratio increased in R3 (**Figure 3**). In 24% KOH-F, both Ara and Gal decreased in S3 and displayed a peak in R2 with an ensuing decline in R3. Nevertheless, changes in Ara during ripening were smaller in 4 and 24% KOH-F than those occurring in CDTA-F and Na_2CO_3-F. This suggests that diverse Ara populations could be present in different locations of the wall. Ara residues from matrix glycans may be tightly associated with cellulose and could be less susceptible to enzymatic degradation during growth and ripening. Redgwell et al. (*13*) detected high molecular weight pectic arabinogalactans very strongly associated with cellulose in many fruit species. In peach, Brummell et al. (*10*) also found a substantial polyuronide component in the alkali extracts eluting in the void volume of the size exclusion column. The sugar composition data for the two matrix glycan extracts also support the view that xyloglucans are much more abundant cell wall constituents than xylans in the Japanese plum (**Figure 3**). Because Xyl represents higher mole percent than Glc in the 4% KOH-F (and a similar proportion in 24% KOH-F), small amounts of xylans may be obtained from this extract.

Massive losses of cell wall Ara occur in both peaches and Japanese plums, but the mechanisms seem to differ. In peach, α-L-arabinofuranosidase/β-D-xylosidase (*PpARF/XYL*) and α-L-arabinofuranosidase (*PpARF1*) genes showed to be expressed during peach ripening, with maximum transcript levels at the end of the climacteric rise and during the melting period of softening, respectively (*30*). This agrees with previous findings regarding substantial losses of Ara from loosely bound matrix glycans in those stages and an increase in the polymeric Ara content of the CDTA-soluble fraction (*10*). Besides, α-L-arabinofuranosidase/β-D-xylosidase and α-L-arabinofuranosidase genes have been partially cloned from 'Gigaglia' plum and found to be expressed during fruit ripening (M. C. Di Santo, E. A. Pagano, and G. O. Sozzi, unpublished data). Because a massive loss of Ara from pectic fractions, but not from matrix glycans, was detected in this work, these enzymes could play a role in pectin disassembly by stripping the rhamnogalacturonan side chains rich in Ara. A similar role has been suggested for the ethylene-modulated α-arabinofuranosidase III from tomato fruit, which is capable of releasing free Ara from Na_2CO_3-soluble pectins (*20*).

In conclusion, examination of six developmental stages allowed a better understanding of the biochemistry of cell wall

degradation in *P. salicina* Lindl. A drastic decrease in the Ara/Gal ratio in tightly bound (Na_2CO_3-F) pectins (**Figure 3**) and the beginning of depolymerization of matrix glycans (**Figure 5**) take place at the end of the cell expansion phase (S3), thus suggesting that these events may be early contributors to fruit softening. Early ripening (R1) is marked by the sustained depolymerization of matrix glycans and increased pectin solubilization. Late ripening (R3) is characterized by a strong depolymerization of cell wall polyuronides and matrix glycans as well as a decrease in the Ara/Gal ratio in loosely bound (CDTA-F) pectins. Additionally, this work proves the unfeasibility of considering the European plum cell wall as a model applicable to Japanese plum.

ABBREVIATIONS USED

AIR, alcohol-insoluble residue; Ara, arabinose; CDTA, *trans*-1,2-diaminocyclohexane-*N*,*N*,*N*′,*N*′-tetraacetic acid; CDTA-F, CDTA-soluble fraction; DAA, days after anthesis; FID, flame ionization detector; Fuc, fucose; Gal, galactose; GalA, galacturonic acid; Glc, glucose; *h*°, hue angle; HPLC, high-performance liquid chromatography; 4% KOH-F, 4% KOH-soluble fraction; 24% KOH-F, 24% KOH-soluble fraction; Man, mannose; Na_2CO_3-F, Na_2CO_3-soluble fraction; R1 early ripe; R2, midripe; R3, fully ripe; Rha, rhamnose; S1, initial phase of exponential growth; S2, lag phase; S3, end of the cell expansion phase; SEC, size exclusion chromatography; TCD, thermal conductivity detector; TFA, trifluoroacetic acid; W-F, water-soluble fraction; Xyl, xylose.

ACKNOWLEDGMENT

The aid of Dr. Diego A. Navarro in setting up the HPLC is gratefully acknowledged.

LITERATURE CITED

(1) Okie, W. R. *Prunus domestica* (European plum) − *Prunus salicina* (Japanese plum). In *The Encyclopedia of Fruit and Nuts*; Janick, J., Paull, R. E., Eds.; CABI: Wallingford, Oxfordshire, U.K., 2008; pp 694−705.

(2) Srinivasan, C.; Padilla, I. M. G.; Scorza, R. *Prunus* spp. Almond, apricot, cherry, nectarine, peach and plum. In *Biotechnology of Fruit and Nut Crops*; Litz, R. E., Ed.; CABI Publishing: Wallingford, Oxfordshire, U.K., 2005; pp 512−542.

(3) Cosgrove, D. J. Relaxation in a high-stress environment: the molecular basis of extensible cell walls and cell enlargement. *Plant Cell* **1997**, *9*, 1031–1041.

(4) Brummell, D. A. Cell wall disassembly in ripening fruit. *Funct. Plant Biol.* **2006**, *33*, 103–119.

(5) Bennett, A. B.; Labavitch, J. M. Ethylene and ripening-regulated expression and function of fruit cell wall modifying proteins. *Plant Sci.* **2008**, *175*, 130–136.

(6) Goulao, L. F.; Oliveira, C. M. Cell wall modifications during fruit ripening: when a fruit is not the fruit. *Trends Food Sci. Technol.* **2008**, *19*, 4–25.

(7) Hiwasa, K.; Nakano, R.; Hashimoto, A.; Matsuzaki, M.; Murayama, H.; Inaba, A.; Kubo, Y. European, Chinese and Japanese pear fruits exhibit differential softening characteristics during ripening. *J. Exp. Bot.* **2004**, *55*, 2281–2290.

(8) Gross, K. C.; Sams, C. E. Changes in cell wall neutral sugar composition during fruit ripening: a species survey. *Phytochemistry* **1984**, *23*, 2457–2461.

(9) Bouranis, D. L.; Niavis, C. A. Cell wall metabolism in growing and ripening stone fruits. *Plant Cell Physiol.* **1992**, *33*, 999–1008.

(10) Brummell, D. A.; Dal Cin, V.; Crisosto, C. H.; Labavitch, J. M. Cell wall metabolism during maturation, ripening and senescence of peach fruit. *J. Exp. Bot.* **2004**, *55*, 2029–2039.

(11) Dawson, D. M.; Melton, L. D.; Watkins, C. B. Cell wall changes in nectarines (*Prunus persica*). Solubilization and depolymerization of pectic and neutral polymers during ripening and in mealy fruit. *Plant Physiol.* **1992**, *100*, 1203−1210; correction in *Plant Physiol.* **1993**, *102*, 1062−1063.

(12) Redgwell, R. J.; MacRae, E.; Hallett, I.; Fischer, M.; Perry, J.; Harker, R. In vivo and in vitro swelling of cell walls during fruit ripening. *Planta* **1997**, *203*, 162–173.

(13) Redgwell, R. J.; Fischer, M.; Kendal, E.; MacRae, E. A. Galactose loss and fruit ripening: high-molecular-weight arabinogalactans in the pectic polysaccharides of fruit cell walls. *Planta* **1997**, *203*, 174–181.

(14) Renard, C. M. G. C.; Ginies, C. Comparison of the cell wall composition for flesh and skin from five different plums. *Food Chem.* **2009**, *114*, 1042–1049.

(15) Taylor, M. A.; Rabe, E.; Dodd, M. C.; Jacobs, G. Effect of storage regimes on pectolytic enzymes, pectic substances, internal conductivity and gel breakdown in cold stored 'Songold' plums. *J. Hortic. Sci.* **1994**, *69*, 527–534.

(16) Manganaris, G. A.; Vicente, A. R.; Crisosto, C. H.; Labavitch, J. M. Cell wall modifications in chilling-injured plum fruit (*Prunus salicina*). *Postharvest Biol. Technol.* **2008**, *48*, 77–83.

(17) Trinchero, G. D.; Sozzi, G. O.; Cerri, A. M.; Vilella, F.; Fraschina, A. A. Ripening-related changes in ethylene production, respiration rate and cell-wall enzyme activity in goldenberry (*Physalis peruviana* L.), a solanaceous species. *Postharvest Biol. Technol.* **1999**, *16*, 139–145.

(18) Sozzi, G. O.; Abraján-Villaseñor, M.; Trinchero, G. D.; Fraschina, A. A. Postharvest response of 'Brown Turkey' figs (*Ficus carica* L.) to the inhibition of ethylene perception. *J. Sci. Food Agric.* **2005**, *85*, 2503−2508.

(19) Sozzi, G. O.; Trinchero, G. D.; Fraschina, A. A. Delayed ripening of 'Bartlett' pears treated with nitric oxide. *J. Hortic. Sci. Biotechnol.* **2003**, *78*, 899–903.

(20) Sozzi, G. O.; Greve, L. C.; Prody, G. A.; Labavitch, J. M. Gibberellic acid, synthetic auxins, and ethylene differentially modulate α-L-arabinofuranosidase activities in antisense 1-aminocyclopropane-1-carboxylic acid synthase tomato pericarp discs. *Plant Physiol.* **2002**, *129*, 1330–1340.

(21) Ponce, N. M. A.; Pujol, C. A.; Damonte, E. B.; Flores, M. L.; Stortz, C. A. Fucoidans from the brown seaweed *Adenocystis utricularis*: extraction methods, antiviral activity and structural studies. *Carbohydr. Res.* **2003**, *338*, 153–165.

(22) El-Sharkawy, I.; Kim, W. S.; El-Kereamy, A.; Jayasankar, S.; Svircev, A. M.; Brown, D. C. W. Isolation and characterization of four ethylene signal transduction elements in plums (*Prunus salicina* L.). *J. Exp. Bot.* **2007**, *58*, 3631–3643.

(23) Brummell, D. A.; Labavitch, J. M. Effect of antisense suppression of endopolygalacturonase activity on polyuronide molecular weight in ripening tomato fruit and in fruit homogenates. *Plant Physiol.* **1997**, *115*, 717–725.

(24) Huber, D. J.; O′Donoghue, E. M. Polyuronides in avocado (*Persea americana*) and tomato (*Lycopersicon esculentum*) fruits exhibit markedly different patterns of molecular weight downshifts during ripening. *Plant Physiol.* **1993**, *102*, 473–480.

(25) Rose, J. K. C.; Hadfield, K. A.; Labavitch, J. M.; Bennett, A. B. Temporal sequence of cell wall disassembly in rapidly ripening melon fruit. *Plant Physiol.* **1998**, *117*, 345–361.

(26) O′Donoghue, E. M.; Huber, D. J. Modification of matrix polysaccharides during avocado (*Persea americana*) fruit ripening: an assessment of the role of C_x-cellulase. *Physiol. Plant.* **1992**, *86*, 33–42.

(27) Redgwell, R. J.; Melton, L. D.; Brasch, D. J. Cell-wall polysaccharides of kiwifruit (*Actinidia deliciosa*): effect of ripening on the structural features of cell-wall materials. *Carbohydr. Res.* **1991**, *109*, 191–202.

(28) Cutillas-Iturralde, A.; Zarra, I.; Fry, S. C.; Lorences, E. P. Implication of persimmon fruit hemicellulose metabolism in the softening process. Importance of xyloglucan endotransglycosylase. *Physiol. Plant.* **1994**, *91*, 169–176.

(29) Tong, C. B. S.; Gross, K. C. Glycosyl-linkage composition of tomato fruit cell wall hemicellulosic fractions during ripening. *Physiol. Plant.* **1988**, *74*, 365–370.

(30) Di Santo, M. C.; Pagano, E. A.; Sozzi, G. O. Differential expression of α-L-arabinofuranosidase and α-L-arabinofuranosidase/β-D-xylosidase genes during peach growth and ripening. *Plant Physiol. Biochem*. **2009**, *47*, 562–569.

Received for review November 6, 2009. Revised manuscript received January 8, 2010. Accepted January 9, 2010. We thank the Consejo Nacional de Investigaciones Científicas y Técnicas, the Universidad de Buenos Aires (UBACyT Program), and the Agencia Nacional de Promoción Científica y Tecnológica (PICT 2006-01267) for financial support. This work was carried out with the aid of a postdoctoral fellowship from CONICET granted to N.M.A.P. under the direction of G.O.S. V.H.Z. is an addressee of a doctoral fellowship from the "Programas de Formación de Doctores en Áreas Tecnológicas Prioritarias PMT 111 - PFDT N° 1-5" (UBA-ANPCyT).